JTTEE5 16:374–380
DOI: 10.1007/s11666-007-9045-4
1059-9630/$19.00 © ASM International

Peer Reviewed

Microstructure of Advanced TiC-Based Coatings Prepared by Laser Cladding

Anja Techel, Lutz-Michael Berger, and Steffen Nowotny

(Submitted August 11, 2006; in revised form April 24, 2007)

The specific advantages of TiC as a hard material are its low density, high hardness, and its high alloyability in metal matrix composites. Agglomerated and sintered core-rim structured TiC-based powders were intensively studied in the last few years for thermal spray coating solutions. In the work described in this paper a powder with cubic (Ti,Mo)(C,N) hard phases and Co binder were used together with mechanically mixed NiBSi and CoCrMo powders to produce wear resistant coatings by laser cladding. Coatings with fine-grained hard particles were obtained. Basic process parameters and coating microstructures are described.

Keywords laser cladding, surface protection, system technology, TiC-based hardmetal coatings

1. Introduction

Application of coatings by laser surfacing is widely used in order to increase the wear resistance of new machine components or for repair purposes. Typical hard materials and composites for laser surfacing are WC and WC/W_2C (Ref 1-4). They are mostly applied together with mechanically mixed self-fluxing Ni-based alloys. In the result, composite structures with about 50% coarse-grained hard particles in a ductile binder are produced. These coatings are characterized by a very high resistance against abrasive wear with coarse particles. Multiple metallurgical reactions of WC and W_2C in the molten bath prevent the realization of fine-grained welded structures. For this reason numerous development activities were directed to the realization of fine-grained structures by alternative hard phases, in particular by vanadium carbide (VC) (Ref 5-7).

For different industrial applications VC is used with a steel-based binder matrix. Fine-grained carbides can be prepared by laser surfacing using agglomerated and sintered powders. Dissolved VC does not show metallurgical reactions and formation of new phases with the binder. It precipitates as monocarbide in the form of small dendrites. Therefore, VC is easily processable by welding processes. Coatings show a high ductility and a poor propensity to crack formation.

A comparison of the physical properties of TiC with those of WC, and Cr_3C_2 (Ref 8) and results of fundamental research on phase equilibria and metallurgical reactions of TiC-based composite materials (Ref 9) were the driving forces to use alloyed, core-rim structured TiC-based materials for the development of thermal spray coating solutions (Ref 10, 11). The core-rim structure is formed during the sintering step of spray powder preparation as a result of metallurgical reactions occurring between the starting components, TiC, Mo_2C, Ni and/or Co on the one hand and $TiC_{0.7}N_{0.3}$, Mo_2C, Ni and/or Co on the other (see Fig. 1). The integral compositions for both alloying steps are best described by the general formulas (Ti,Mo)C-NiCo or (Ti,Mo)(C,N)-NiCo. The main function of Mo as an alloying element is the improvement of wetting between the hard phase and binder, while the function of N is the grain growth inhibition of the core-rim structured hard phase grains. The spray coating properties, e.g. abrasion wear resistance, were significantly improved compared to the simple binary TiC-Ni coatings (Ref 11, 12).

Coarse titanium carbide particles were successfully proved for laser cladding (Ref 13). The aim of the experiments described in this work, was the preparation of fine-grained structures in coatings prepared by laser surfacing from an experimental (Ti,Mo)(C,N)-Co surfacing powder, mechanically mixed with a NiBSi or CoCrMo powder. The appearance of a strong metallurgical bonding between the substrate and the coating and a higher coating thickness are general advantages of the welding processes.

2. Experimental

2.1 Coating Powder Preparation and Characterization

The (Ti,Mo)(C,N)-Co powder was prepared by agglomeration and sintering at Fh-IKTS starting from 59.5 wt.% $TiC_{0.7}N_{0.3}$, 12 wt.% Mo_2C, and 28.4 wt.% Co. In the resulting powder, the binder content corresponds to about 20 vol.%. As described above, during the sintering

Anja Techel, Lutz-Michael Berger, and **Steffen Nowotny,** Fraunhofer Institute for Material and Beam Technology (Fh-IWS), Winterbergstrasse 28, 01277, Dresden, Germany. Contact e-mail: Anja.Techel@iws.fraunhofer.de.

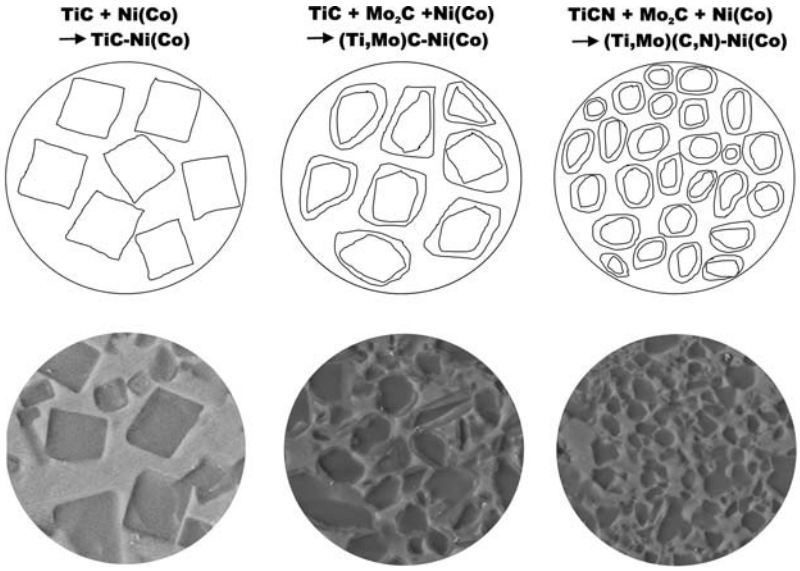

Fig. 1 Formation of core-rim structured (Ti,Mo)C-NiCo and (Ti,Mo)(C,N)-NiCo powders

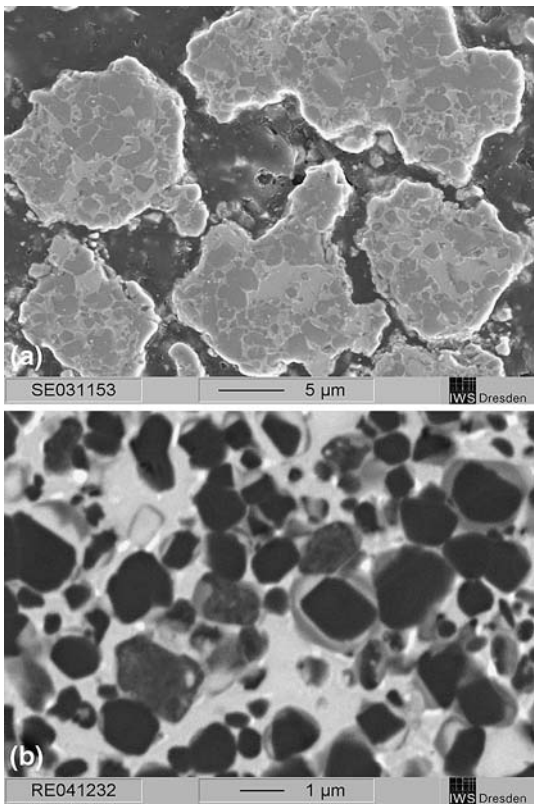

Fig. 2 (a) SEM micrograph of the cross-section of a (Ti,Mo)(C, N)-Co powder. (b) High-resolution SEM micrograph of the cross-section of a (Ti,Mo)(C, N)-Co powder particle

step in spray powder preparation the phase composition changes as a result of metallurgical reactions (Mo_2C is fully depleted in these reactions) and the typical core-rim structure of the cubic hard phases is formed. Figure 2a and b shows the SEM micrographs of the cross-sections of the (Ti,Mo)(C,N)-Co powder.

The x-ray diffraction pattern of the powder was measured as described below for the coatings. In the powder the cubic hard phases with coinciding lattice parameters and the cubic binder phase were detected (see Fig. 6, 10). The lattice parameters of the coinciding cubic hard phases and cubic binder phase of the (Ti,Mo)(C,N)-Co powder were determined with 0.4294 and 0.3561 nm, respectively.

The nominal powder particle size used was $-90+45$ µm. Directly during the surfacing processes the (Ti,Mo)(C,N)-Co powder was mixed with a NiBSi or CoCrMo powder (Deloro Stellite GmbH, see Table 1) with a nominal particle size $-90+45$ µm. The powders were mixed with a ratio of about 2:1 by weight for prevention of crack formation.

2.2 Laser Surfacing Processes

The laser surfacing experiments were performed with a CNC machine using a Nd:YAG-Laser (Rofin Sinar) with a maximum laser power of 4 kW. A powder feeder Twin 10C (Plasmatechnik AG, Wohlen, Switzerland) was used for the powder supply. Figure 3 shows the system technique for laser welding experiments.

For realization of a continuous coaxial powder supply into the melted bath a powder nozzle was used, which has been developed for this purpose at Fh-IWS (see Fig. 4).

Table 1 Chemical compositions of the metal powders used for blending with (Ti,Mo)(C,N)-Co

wt.%	Ni	Co	Fe	B	C	Si	Mn	Mo	Cr
NiBSi	96.4			1.3		2.3			
CoCrMo	2.5	59.5	2.75		0.25	1.5	1	5.5	27

This powder nozzle has a special chamber to mix powders and regulate the particle velocity (Ref 14).

Coatings were deposited directly onto cleaned steel substrates (material numbers 1.0503 and 1.0037 according to the European standard DIN EN 10027-2) by laser cladding. Optimized parameter sets for laser cladding of (Ti,Mo)(C,N)-Co with different binder materials are compiled in Table 2. Carrier gas for the process was argon. The coated surfaces are characterized by uniform and slightly wavy shape.

Fig. 3 Automated system for laser welding experiments

Fig. 4 Coaxial powder nozzle for laser welding experiments

Table 2 Laser surfacing process parameters

Hardmetal powder	(Ti,Mo)(C,N)-Co	
Metal binder powder	NiBSi	CoCrMo
Distance between powder nozzle and surface	13 mm	13 mm
Laser power (Nd:YAG)	1500 W	1400 W
TiC-based powder mass flow	2.5 g/min	2.5 g/min
Metal powder mass flow	1.5 g/min	1.5 g/min
Welding velocity	600 mm/min	400 mm/min
Single layer width	2 mm	2.5 mm
Single layer thickness	0.4 mm	0.4 mm
Offset per layer	1 mm	1 mm

For the characterization of the microstructures two-dimensional claddings were produced with a fixed nozzle and a meander traverse path. Substrate dimensions were suitable for the different characterization procedures.

2.3 Coating Characterization

Coating microstructures were studied using optical and SEM micrographs of metallographically prepared cross-sections. Hardness testing was performed with a Vickers microhardness tester using a 300 g load. The phase compositions of the powders and the coatings were investigated by x-ray diffraction (D8 Advance, Bruker AXS). Measurements were carried out in the θ-2θ step scan mode using Cu Kα radiation with a 2θ range of 15-90° and a step size of 0.05°. In order to study the distribution of the elements in the powder particles, energy-dispersive x-ray (EDX) mapping was performed.

3. Results

3.1 Laser Surfacing with (Ti,Mo)(C,N)-Co and NiBSi

Optical and SEM micrographs of the coating produced by laser welding with (Ti,Mo)(C,N)-Co and NiBSi using the parameter set given in Table 2 are shown in Fig. 5a-c, respectively.

The interface between the coating and substrate is completely free of defects. The distribution of the hard particles in the coating is not in all areas perfectly homogeneous. In the overlapping areas between single tracks, smaller hard particle content than inside the track is observed. The image analysis of a typical coating section inside a single track shows a hard particle content (dark areas) of about 44 vol.%.

The hard phase grains are mostly spheroidal with a grain size predominantly smaller than 5 μm. The average Vickers hardness of about 820 $HV_{0.3}$ with a range between 700 and 1130 $HV_{0.3}$ was measured, depending on the local hard particle content.

The x-ray diffraction pattern in Fig. 6 shows the presence of the cubic hard phases and the cubic metallic binder. The lattice parameter of the binder metal was determined with 0.3550 nm, while the lattice parameter for the cubic hard phases is about 0.4297 nm. Small additional peaks can be attributed to Ni_3B.

The high-magnification SEM micrograph of the coating and the corresponding elemental mappings of Ni, Co, Fe, C, N, Ti, and Mo, are shown in Fig. 7. Ni and Co were mixed during the welding process and form a homogeneous binder alloy, although both metals were fully separated in the mechanically mixed (Ti,Mo)(C,N)-Co and NiBSi starting powders. A significant amount of Fe from the substrate is included in the binder matrix. Ti appears to be concentrated in the hard phase particles only. In the cores of the hard phase grains, no Mo is detected, indicating that this phase represents Ti(C,N). Mo is

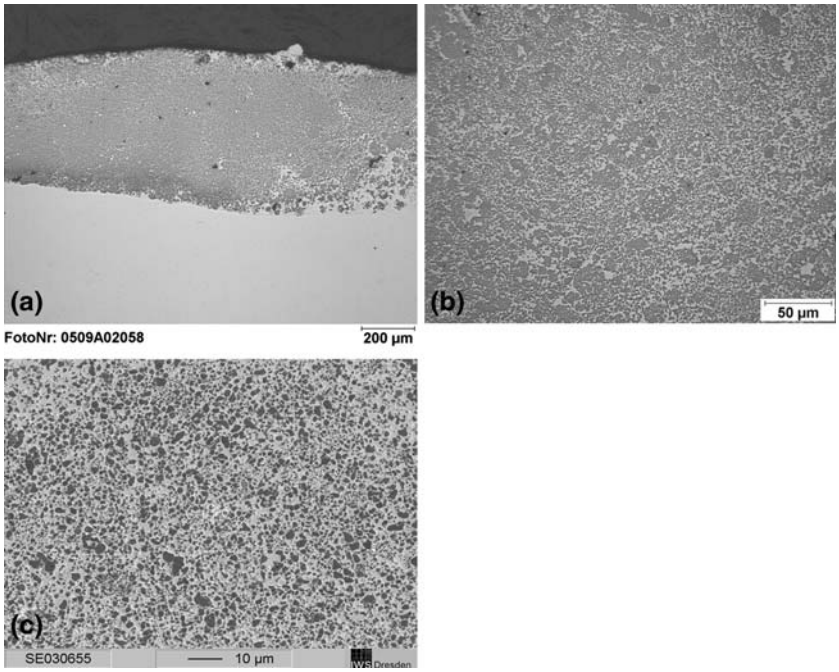

Fig. 5 Optical (a, b) and SEM (c) micrographs of the coating prepared from the mixture of (Ti, Mo)(C,N)-Co and NiBSi powders

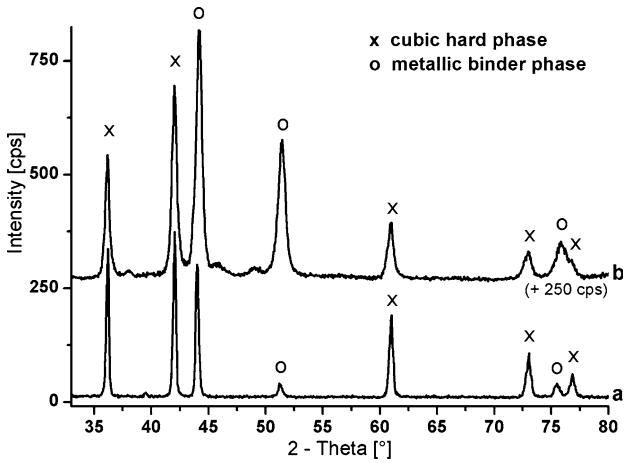

Fig. 6 X-ray diffraction patterns of the (Ti,Mo)(C,N)-Co powder (line *a*) and the coating produced from this powder and the NiBSi powder (line *b*)

concentrated in the rims of these core-rim structured grains, and in few smaller grains at the edges of investigated section. Other small hard phase grains, appearing dark in SEM micrograph, seem to consist of Ti, C, and N only. The content of N in the cores is significantly higher than in the rims.

3.2 Laser surfacing with (Ti,Mo)(C,N)-Co and CoCrMo

Optical and SEM micrographs of the coating produced by laser welding with (Ti,Mo)(C,N)-Co and CoCrMo using the parameter set given in Table 2 are shown in Fig. 8a-c, respectively.

The transition of the coating to the substrate is completely free of defects. The distribution of the hard particles in the coating is in all areas nearly perfectly homogeneous. The substrate-coating boundary is completely free of defects. The image analysis of a typical coating section inside a single track shows a hard particle content (dark areas) of about 37 vol.% by using an optical microscope image.

After the welding process the hard phase grains are mostly blocky, partially with a starlike shape. This is typical for primary precipitated carbides, which start to grow from a nucleation site. The size of all hard phase grains is smaller than 5 µm. Additionally many carbide grains with sizes smaller than 1 µm have been precipitated. These are probably secondary precipitated carbides from the type TiC or (Ti,Mo)C. If the content of these fine carbides will not be taken into account by using a SEM micrograph the image analysis of the coating section shows only a hard particle content of about 26 vol.%.

An average Vickers hardness of about 500 $HV_{0.3}$ was measured in the coating. The hardness increases continuously from about 420 $HV_{0.3}$ at the coating-substrate boundary to 580 $HV_{0.3}$ at the surface.

The high-magnification SEM micrograph of the coating and the corresponding elemental mappings of Co, Cr, Fe, N, C, Ti, and Mo, are shown in Fig. 9. The Co binder from the hardmetal and the metallic binder were mixed during the welding process. A significant amount of Fe from the substrate is included in the binder matrix. In the mappings all binder elements including Cr and Fe from the molten substrate appear homogeneously distributed. Chromium

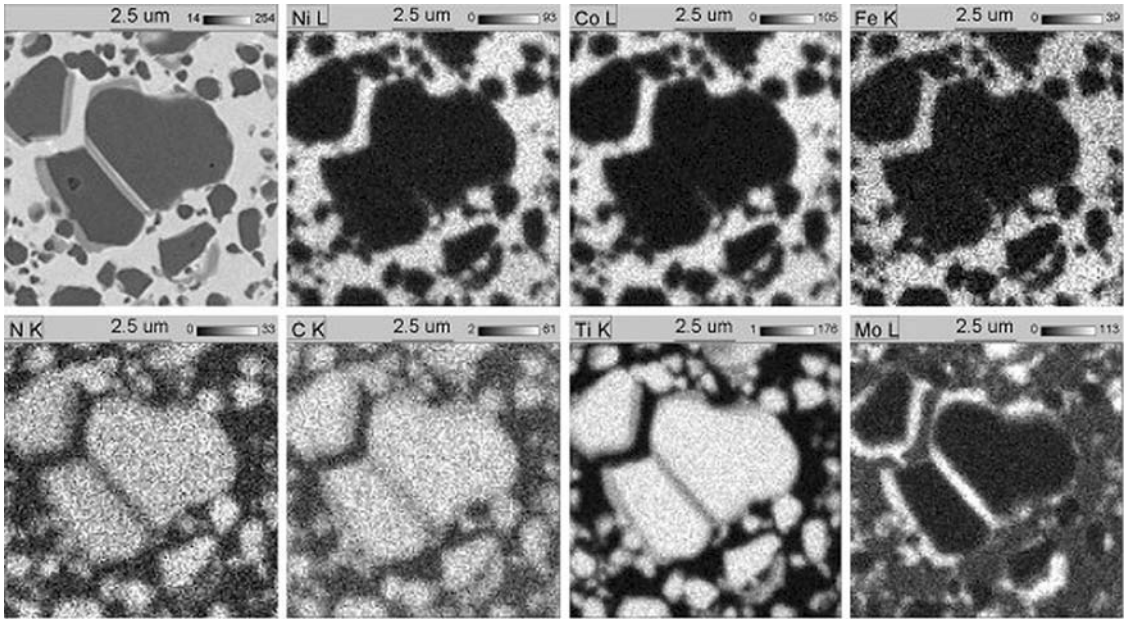

Fig. 7 High-resolution SEM micrograph of the coating (top left) prepared from the mixture of (Ti, Mo)(C,N)-Co and NiBSi powders and corresponding EDX mappings of Ni, Co, Fe, N, C, Ti, and Mo

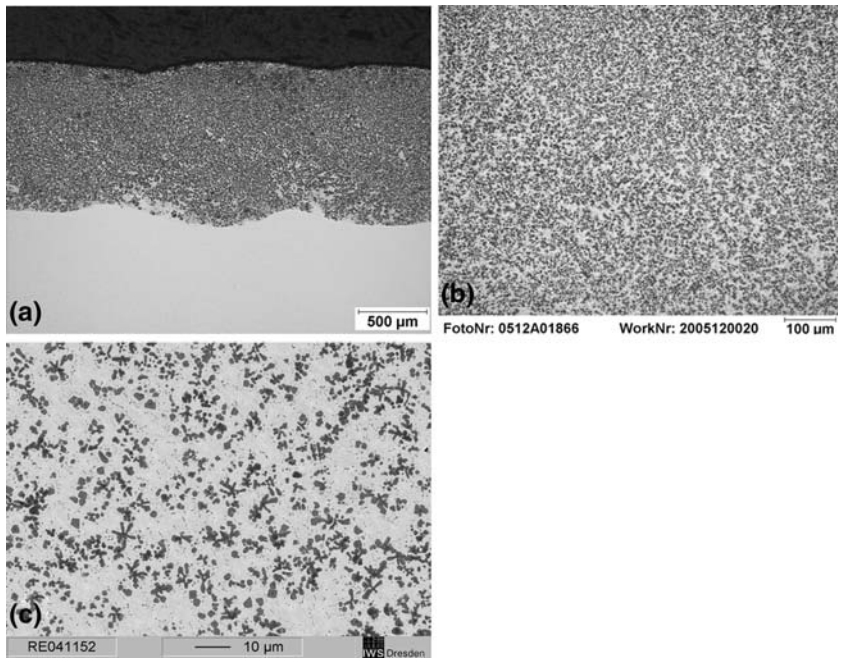

Fig. 8 Optical (a, b) and SEM (c) micrographs of the coating prepared from the mixture of (Ti, Mo)(C,N)-Co and CoCrMo powders

carbide precipitations typical for CoCrMo alloys are not visible yet.

Binder areas with a high content of hard particles smaller than 1 µm show a small rise of the titanium and molybdenum concentration. But these fine particles cannot be detected separately.

The core-rim structure of the hard phase grains is visible in the high-magnification SEM micrograph of the coating and the corresponding elemental mappings of C, N, Ti, and Mo. Ti and C appear to be concentrated in the hard phase particles with a nearly constant concentration. In the cores of the hard phase grains, lower concentration

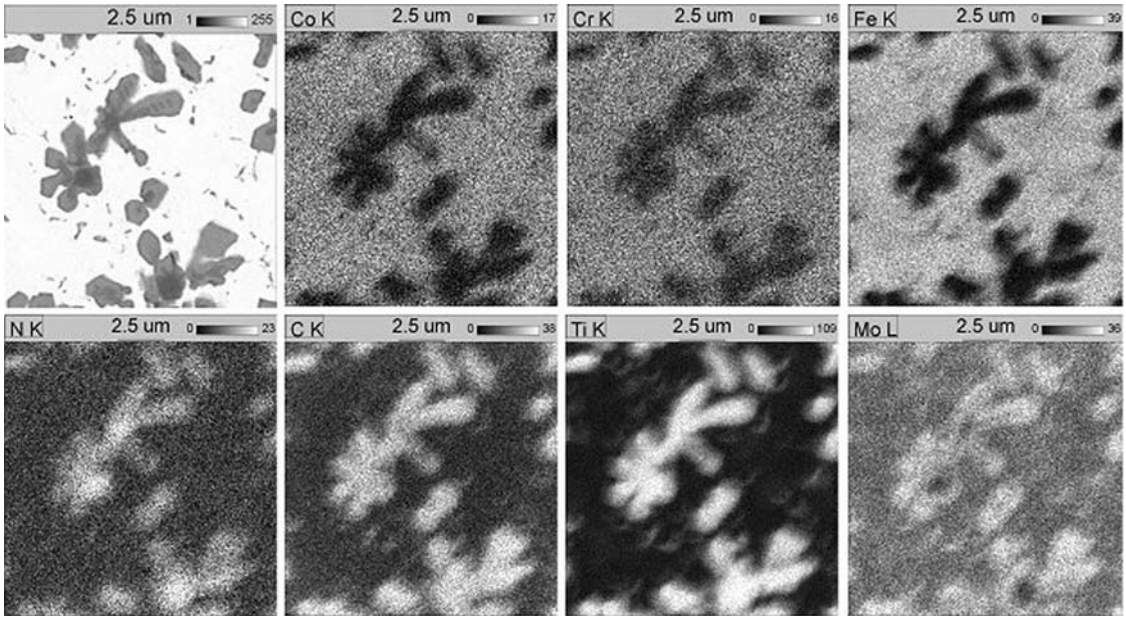

Fig. 9 High-resolution SEM micrograph of the coating (top left) prepared from the mixture of (Ti,Mo)(C,N)-Co and Co-CrMo powders and corresponding EDX mappings of Co, Cr, Fe, N, C, Ti, and Mo

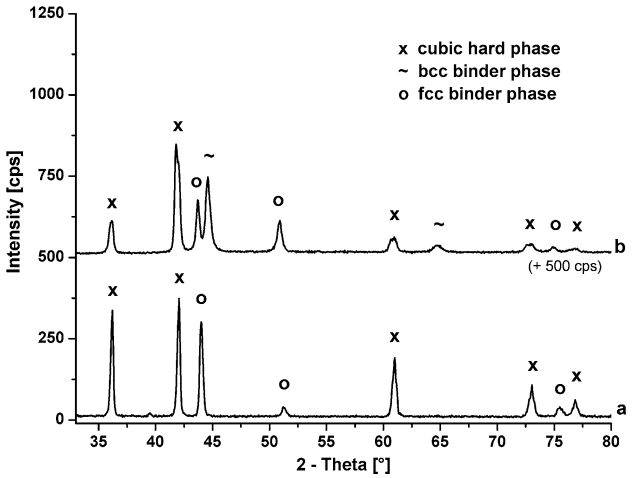

Fig. 10 X-ray diffraction patterns of the (Ti,Mo)(C,N)-Co powder (line *a*) and the coating produced from this powder and the CoCrMo powder (line *b*)

or no Mo is detected, indicating that this phase represents Ti(C,N). In these areas the content of N is significantly higher than that in the rims.

The x-ray diffraction pattern in Fig. 10 shows the presence of the cubic hard phases and in the same range five other peaks. Three of them can be related to the cubic cobalt-based binder originating from metallic binder of hardmetal powder and the blended CoCrMo. The lattice parameter of the cubic hard phases is about 0.4297 nm, while the lattice parameter of the binder metal of the (Ti,Mo)(C,N)-Co powder was determined with 0.3561 nm. In result of the welding process the lattice parameter changes to 0.3584 nm. Despite of the homogeneous appearance of the binder elements in the mappings, the other two peaks can be related to an iron-based binder structure with a lattice parameter of 0.2872.

4. Conclusions

Core-rim structured (Ti,Mo)(C,N)-Co powder prepared by agglomeration and sintering was used to produce laser cladded coatings. For the prevention of crack formation the TiC-based powder was mixed with a NiBSi or CoCrMo powder directly during the surfacing processes. The preparation of fine-grained structures with high hardness and metallurgical bonding to the substrate was demonstrated.

For laser cladding, a full homogenization of the (Ti,Mo)(C,N)-Co powder particles with the mechanically mixed NiBSi binder occurred. The lattice parameter of the cubic metallic binder is influenced by all elements dissolved during the welding process. The lattice parameter of the cubic hard phases has not changed during the welding process. The particle size of the hard phase in the coating is smaller than 5 μm. Hard phase content up to 50 vol.% is reachable. With upcoming work it is expected that the coating hardness can be adjusted in the range of about 500 and 1000 $HV_{0.3}$.

For control of the microstructures of the coatings more work on laser cladding with this powder and more detailed knowledge of the metallurgical reactions with the mechanical mixed binder and the substrate material during the welding process is required. The investigation of mechanical and wear properties will be a topic of further studies.

Acknowledgments

The authors would like to thank colleagues of FhG-IKTS for supplying the (Ti,Mo)(C,N)-Co powder and co-workers, students and technicians of FhG-IWS for the production, metallographic preparation, and microscopic studies of the coatings.

References

1. A. Luft, A. Techel, S. Nowotny, and W. Reitzenstein, Gefügeausbildung beim Laserbeschichten von Stahl mit wolframkarbidverstärkten Nickelhartlegierungen (Formation of Microstructure during Laser Cladding of Steel with Nickel Hard Alloys with Tungsten Carbide Reinforcements), *Schweißen Schneiden*, 1995, **47**(2), p 124-132 (in German)
2. A. Luft, A. Techel, S. Nowotny, and W. Reitzenstein, Microstructures and Dissolution of Carbides Occuring During the Laser Cladding of Steel with Tungsten Carbide Reinforced Ni- and Co-Hard Alloys, *Prakt. Met.*, 1995, **32**(No 5), p 235-247
3. A. Techel, A. Luft, A. Müller, and S. Nowotny, Production of Hard Metal-Like Wear Protection Coatings by CO_2 Laser Cladding, *Opt. Quantum Electron.*, 1995, **27**, p 1313-1318
4. B. Bouaifi, A. Gebert, and I. Aydin, Schutzschichten mit beanspruchungsgerechter Hartstoffeinlagerung (Protective Coatings with Load-Relevant Hard Phase Inclusions), *DVS-Berichte*, Vol. 237, DVS-Verlag, 2005, p 332-337 (in German)
5. H. Heinze, A. Gebert, B. Bouaifi, and A. Ait-Mekideche, Korrosionsbeständige Auftragschweißschichten auf Eisenbasis mit hoher Verschleißbeständigkeit (Corrosion Resistant Iron-Based Welded Coatings with High Wear Resistance), *Schweißen Schneiden*, 1999, **51**(9), p 550-555 (in German)
6. A. Gebert, B. Bouaifi, and E. Teupke, Neue vanadinkarbidhaltige Schweißzusätze zum Schutz gegen Verschleiß und Korrosion (New Feedstock Materials on the Base of Vanadium Carbide for Protection against Wear and Corrosion), *DVS-Berichte*, Vol. 216, DVS-Verlag, 2001, p 365-370 (in German)
7. B. Bouaifi, U. Draugelates, A. Gebert, and H. Küpper, Standzeitverbesserung durch Einsatz vanadinkarbidhaltiger Nickelbasis-Schutzschichten (Increase of Service Life by Use of Vanadium Carbide-Containing Nickel-Based Coatings), *HTM Z. Werkst. Wärmebeh. Fertigung*, 2004, **59**(5), p 329-334 (in German)
8. L.-M. Berger, W. Hermel, P. Vuoristo, T. Mäntylä, W. Lengauer, and P. Ettmayer, Structure, Properties and Potentials of WC-Co, Cr_3C_2-NiCr and TiC-Ni-Based Hardmetal-Like Coatings, *Thermal Spray: Practical Solutions for Engineering Problems*, C.C. Berndt, Ed., ASM International, 1996, p 89-96
9. P. Ettmayer and W. Lengauer, The Story of Cermets, *Powder Met. Int.*, 1989, **21**(2), p 37-38
10. L.-M. Berger, M. Nebelung, P. Vuoristo, and T. Mäntylä, *Coating Powder and Method for its Production*, DE 196 40 788 (filing date: 02 Oct 1996), WO 98/14630, US 6 162 276, EP 0948659, CA 2 267 960, BR 9711858-3, NO 321957
11. L.-M. Berger, S. Thiele, P. Vuoristo, T. Mäntylä, H. Keller, E. Proß, and R. Scholl, Titanium Carbide-Based Powders and Coatings—Compositions, Processability and Properties, *Int. Thermal Spray Conf. 2002*, E. Lugscheider and C.C. Berndt, Ed., DVS-Verlag, 2002, p 727-732
12. P. Vuoristo, T. Mäntylä, L.-M. Berger, and M. Nebelung, Sprayability and Properties of TiC-Ni Based Powders in the Detonation Gun and HVOF Processes, *Thermal Spray: A United Forum for Scientific and Technological Advances*, C.C. Berndt, Ed., Sept 15-18, 1997 (Indianapolis, IN), ASM International, 1998, p 909-915
13. K. Nakata, H. Nakagura, Y. Honda, and S. Tomida, Laser Cladding of TiC Dispersed Ni-Cr Composite Layer on Carbon Steel, *Trans. JWRI*, 1997, **26**(2), p 91-93
14. S. Nowotny and S. Scharek, Machining Head and Process for the Surface Machining of Workpieces by Means of a Laser Beam, DE 199 09 390 (filing date: 4 March 1999), US 6 316 744